FORWARD MODELING OF THE INDUCTION LOG RESPONSE OF A FRACTURED GEOLOGIC FORMATION

A Thesis

by

STEVEN HUNTER BRAY

Submitted to the Office of Graduate Studies of
Texas A&M University
in partial fulfillment of the requirements for the degree of

MASTER OF SCIENCE

Approved by:

Chair of Committee,	Mark Everett
Committee Members,	Yuefeng Sun
	Zoya Heidari
Head of Department,	Rick Giardino

May 2013

Major Subject: Geophysics

ABSTRACT

Induction logging is a well-developed geophysical method with multiple applications. It has been used extensively in academic research as well as in industry. Induction logging is a controlled-source electromagnetic (CSEM) exploration method. It characterizes geologic formations through the measurements of induced magnetics fields. The purpose of this research project is to better understand induction logs and the effects fractured geologic formations have on them.

Computer modeling is used to generate synthetic logs for analysis in this research project. The original program required certain modifications to fit this research project's goals. The computer program, Seatem is based on the finite element method. It is able to use a layered Earth model that is the basis for the synthetic log analysis. The geologic layers in this model are assigned various conductivities and also have the option of being assigned a geologic roughness value. The geologic roughness parameter is used to simulate fractured rocks in the subsurface.

The synthetic logs generated by the modified Seatem program produce some encouraging results. In a thinning bed analysis, it is shown that as a conductive bed is thinned in a step-size procedure, the resulting induction log underestimates the actual conductivity of the layer. It also shows that the boundary layers around the thinned layer are better characterized in the log. The next synthetic log was calculated for a fractured resistive layer. This log

shows that as the layer becomes more fractured, there is an increase in the underestimation of the actual conductivity. This layer is then thinned down and another synthetic log is calculated. The resulting log shows similar traits to the thinning bed analysis and shows an underestimation of the apparent conductivity. The same procedure is performed for a fractured conductive layer. The analysis produce similar results; however, that are much more drastic changes in the induction logs. As the unit becomes more fractured, the apparent conductivity is lower then the actual conductivity, as in the resistive case. However, smaller increases in the roughness parameter produced more severe underestimations than larger increases in the roughness parameter did for the resistive layer.

ACKNOWLEDGEMENTS

There are many people that I owe a great deal of thanks to who have been supportive of me during my higher education. First, and foremost, I would to thank my family, especially my parents. Without their encouragement, love and support, none of what I have achieved to date would be possible. They have always inspired me to be the best person I can be, and I can't thank them enough for their example in my life.

My research goals would not be achievable without the great deal of support and effort from my graduate advisor, Dr. Everett. Dr. Everett's instruction and support over the past five years has, without a doubt, made my undergraduate and graduate career possible. I am very thankful for his insight as a professor and I look forward to having him as a colleague in the future.

Many others deserve my gratitude in relation to this project. My committee members Dr. Yuefeng Sun and Dr. Zoya Heidari have been very supportive during my thesis work and I thank them for that. I would also like to thank the near-surface research group for their input on my thesis work.

Lastly, I would like to think the Berg Hughes Center for the use of their computer technology. They have been a great resource and, without their help, this project would not be possible.

NOMENCLATURE

CSEM	Controlled-source Electromagnetics
EM	Electromagnetic
FE	Finite Element
MI	Multicomponent Induction
QMR	Quasi-minimal Residual
Rx	Receiver
Tx	Transmitter

TABLE OF CONTENTS

LIST OF FIGURES

1. INTRODUCTION

Induction logging has become a valuable tool in the evaluation of geologic formations over the past half-century. Induction logging uses an electromagnetic loop source that is inductively coupled to the surrounding geological strata. The source does not require contact with the wellbore or geologic formation (Doll, 1949). As the transmitter generates an electromagnetic field, the receiver component of the logging tool measures the response of the formation, which is sensitive to the electrical conductivity of the formation in addition to various other factors related to the borehole. The measurement is converted into an apparent conductivity, typically presented as a log and corresponds to a fixed transmitter frequency in the range of 100Hz to 1MHz. The tool is moved along the wellbore while the receiver measures the response from the traversed formations (Doll, 1949).

As the technology for evaluating geologic formations becomes more advanced, certain characteristics of the subsurface can be explored in greater detail. One such characteristic is the fracture density of a formation. Mainly driven by petroleum industry concerns, determining fracture density has become very important in reservoir evaluation. With drilling techniques becoming more complex and unconventional, the goal of understanding the behavior of fractured media is becoming increasingly important in hydrocarbon production. With the steep rise in popularity of shale gas, for example, hydraulic fracturing is often used to recover hydrocarbons. Greater insight to

the outcomes of hydraulic fracturing can lead to better production and better understanding of its potential environmental effects. Not only does evaluating fracture density contribute to the successful production of a reservoir, it can also be used in the exploratory phases of prospect assessment. Natural fractures in rocks can contain large hydrocarbon reserves. Comprehending these fractures, and their fill material, can help to forecast the economic viability of a rock unit is for production.

This research project describes a procedure to generate synthetic induction logs with a specific focus on the effect of fractures on geologic formation evaluation. The logs were produced using a forward modeling code written in Fortran and based on the finite element method. The fracturing was modeled using the anomalous electromagnetic diffusion approach first discussed by Weiss and Everett (2007) and a brief analysis of the effects of fracturing was performed.

1.1 Inspiration

Inspiration for this research project came from the analysis of Wang et al. (2005) on characterizing fractures by multicomponent induction (MI) tool measurements. The authors addressed the capability of an MI measurement to detect fractures around the borehole. The fractures were associated with hydraulic fracturing and were studied using both numerical simulation and downhole observations (Wang et al., 2005). Even though the fractures were

caused by hydraulic fracturing, their research method should also be applicable to the characterization of natural fracturing. The MI tool response is sensitive to the fact that hydraulic fractures are filled with fluids of resistivity different from that found within the surrounding formation, thereby producing an azimuthal resistivity anisotropy around the borehole. This difference in resistivity between the mud and the geologic formation allows the MI measurement to resolve the fractures. The measured response of the fractures is heavily dependent on the fracture resistivity and the coil orientation of the induction tool. A schematic of a hydraulic fracture intersecting the cylindrical borehole can be seen in a borehole-perpendicular plane in Figure 1.1.

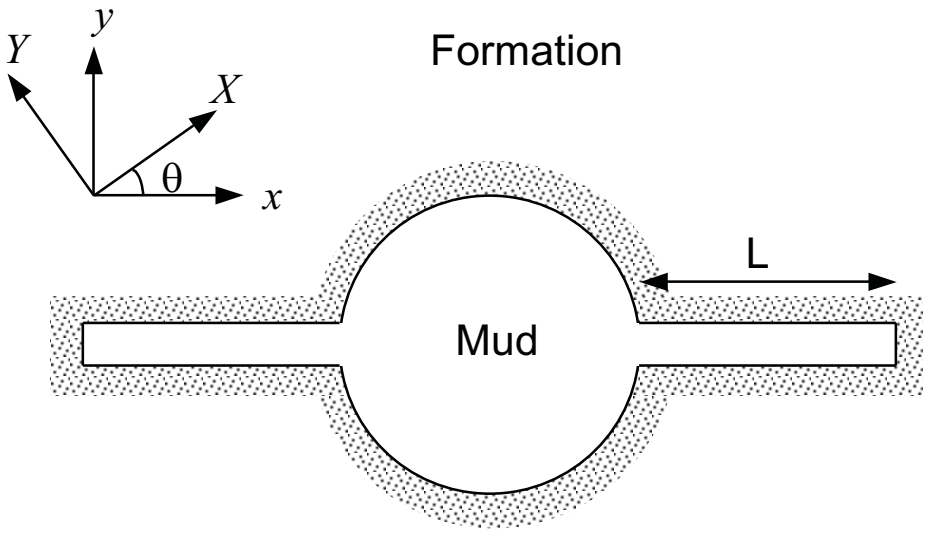

Figure 1.1. A schematic diagram showing, in the x-z plane, a horizontal slice through a wing-like hydraulic fracture . The length L is the fracture length and θ is the angle of azimuthal rotation (Wang et al., 2005).

An induction tool that can measure five different magnetic field components was used by Wang et al. (2005) to identify azimuthal resistivity anisotropy. Once the measurements were taken, the differences between the x and y magnetic components were compared in order to determine fracture length *L*. This analysis found that the greater the difference between the x and y magnetic responses, the greater the fracture length (Wang et al., 2005). The study also determined that fractures filled with conductive fluid were more difficult to resolve then the same fractures filled with resistive fluids. The difficulties in characterizing the conductive fractures were caused by a lack of sensitivity of the magnetic responses in the x and z directions, making the y-directed response the only contributor. After the numerical models were run to determine tool accuracy and reliability, Wang et al. (2005) applied the method to Gulf of Mexico field data with promising results. They were able to establish the existence of fractures around the borehole and, with strong certainty, estimate the length of these fractures.

While the analysis performed by Wang et al. (2005) provided the inspiration for the current research project, my focus on fracture detection and characterization is markedly different. Wang and his colleagues were interested in the azimuthal variations of conductivity readings from MI measurements to resolve hydraulically-induced fracture length around the borehole. I am interested in the effect on apparent conductivity readings from a conventional two-coil vertical induction tool caused by natural fractures in a geologic formation.

2. BACKGROUND

The foundation of induction logging is low-frequency controlled-source electromagnetic (CSEM) induction. The CSEM exploration method can be conceptualized using inductively coupled LR circuits (Grant and West, 1965). A simple diagram of these circuits can be seen in Figure 2.1. This diagram illustrates a primary electromagnetic field, generated by a current flow in the Tx loop, interacting with the Earth or a target of interest, to create a secondary response signal. The total response, primary plus secondary, is measured by the Rx loop. The Rx signal can then be analyzed to determine the physical properties and geometry of the target. Note that the three LR circuits are not directly coupled to each other but rather are magnetically flux-coupled. The flux couplings are described by the mutual inductance M_{ij} parameters.

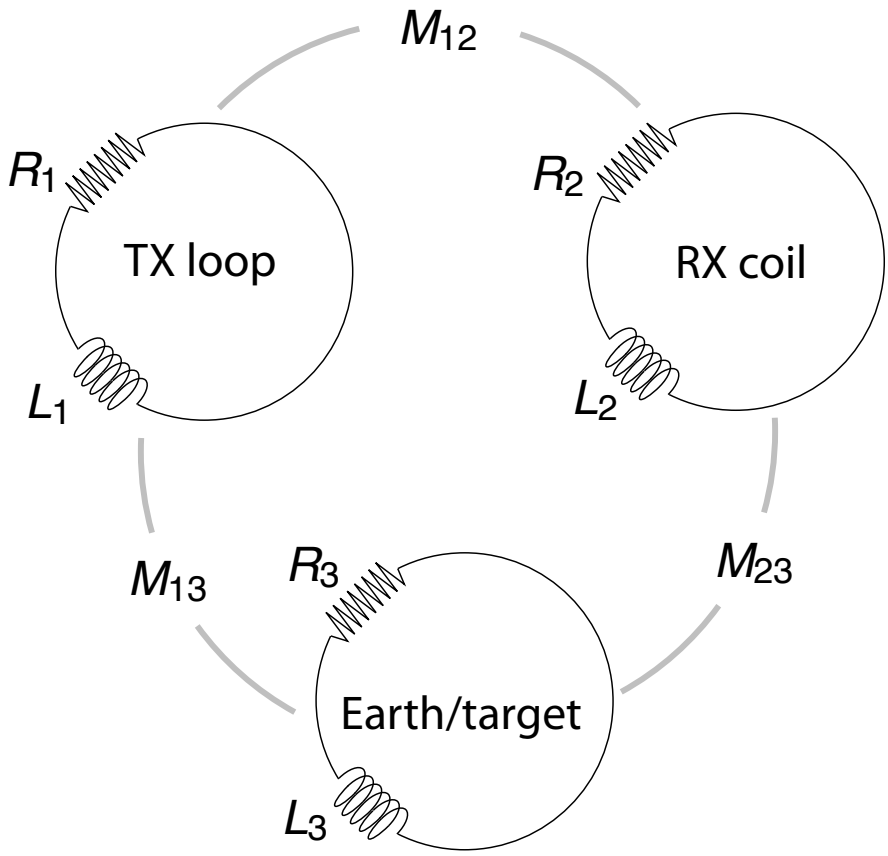

Figure 2.1. A diagram conceptualizing the CSEM exploration method as inductively coupled LR circuits (Grant and West, 1965).

Further understanding is provided by the conceptual diagram shown in Figure 2.2. This diagram depicts the primary and secondary fields that are relevant to CSEM exploration. The Tx is shown generating the primary magnetic field that interacts with the surrounding formation and a conductive target. When the primary field is exposed to its surroundings, a secondary field caused by induced eddy currents is produced. The Rx coil then receives flux from both the primary and secondary magnetic fields and records the resulting signal.

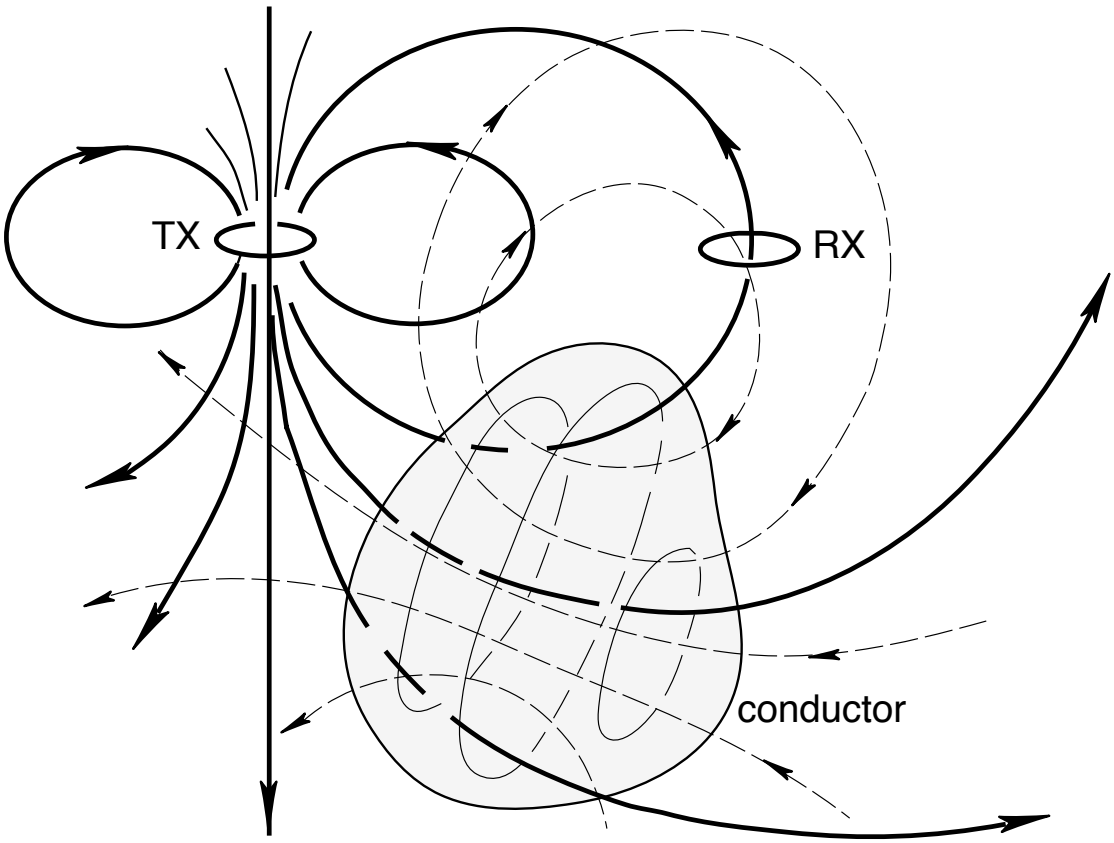

Figure 2.2. A conceptual diagram showing the primary and secondary magnetic fields interacting with a conductive target in a CSEM survey (Everett, 2013).

2.1 Induction Logging Theory

Induction logging uses several coils that encircle an insulating mandrel. For the purposes of this project, a simple two-coil, vertical coaxial system, which can been seen in Figure 2.3, will be assumed. The transmitter coil is energized by an alternating current that induces current flow within the surrounding, conductive earth. The induced currents circulate in closed horizontal loops within the geologic formation. The induced current loops are inductively

coupled (magnetically flux-linked) to each other. The secondary magnetic field generated by the induced current loops, in addition to the primary field of the transmitter, both contribute to a voltage recorded in a separate coil called the receiver. This voltage, containing both in-phase and out-of-phase components with respect to the transmitter current, is measured to produce a signal that is approximately proportional to the formation conductivity (Moran and Kunz, 1962).

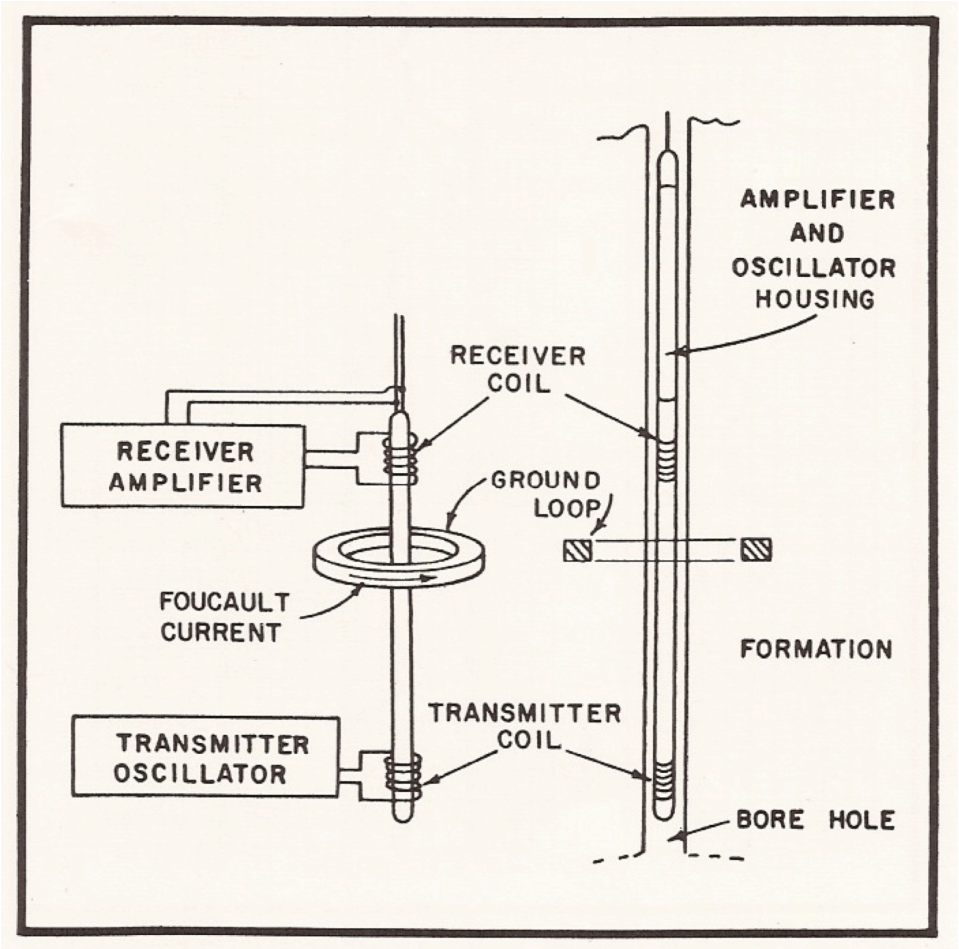

Figure 2.3. Basic two-coil induction system (Schlumberger, 1969).

The formation conductivity can be determined using two methods. The first is an approximation developed by Doll (1949) that involves the use of a geometrical factor. Using 2-D cylindrical coordinates (ρ, z) with azimuthal symmetry, the general equation for the apparent conductivity, σ_g as seen by the induction logging tool is:

$$\sigma_g = \int_{-\infty}^{\infty} dz \int_0^{\infty} g(\rho, z)\sigma(\rho, z)d\rho, \tag{2.1}$$

where $g(\rho, z)$ is the geometrical factor and $\sigma(\rho, z)$ is the formation conductivity (Moran and Kunz, 1962). This method is very simple, but only approximates the full physics of the electromagnetic induction process. Doll (1949) assumes that the induced current in each horizontal layer of a formation circulates independently of the induced currents in adjacent layers; in other words, the induced current loops are not magnetically flux-linked to each other.

Another method used for more accurate modeling takes into better quantitative account physical processes such as the skin effect. This method, as with any detailed induction logging analysis, begins with the governing Maxwell equations:

$$\nabla \times \bar{E} + \frac{\partial \bar{B}}{\partial t} = 0, \tag{2.2}$$

$$\nabla \times \bar{H} + \frac{\partial \bar{D}}{\partial t} = \bar{J}, \tag{2.3}$$

$$\nabla \cdot \bar{B} = 0, \tag{2.4}$$

where $\bar{E}$ is the electric field strength, $\bar{B}$ is the magnetic flux density, $\bar{H}$ is the magnetic field strength, and $\bar{J}$ is the current density (Moran and Kunz, 1962). It must be noted that equation (2.3) contains a $\frac{\partial \bar{D}}{\partial t}$ term describing the so-called displacement current. When applied to induction logging, this term can be safely dropped due to the low induction frequencies that typically run from 1-100 kHz, resulting in the following simplification known as Ampere's law:

$$\nabla \times \bar{H} = \bar{J}. \tag{2.5}$$

The constitutive laws below describe the effect of conductive and magnetic media:

$$\bar{B} = \mu \bar{H}, \tag{2.6}$$

$$\bar{J} = \sigma \bar{E}, \tag{2.7}$$

where μ is magnetic permeability and σ is electrical conductivity. For a layered-Earth analysis to be valid, the material parameters μ and σ must be constant throughout each bed (Moran and Kunz, 1962). Moreover, in conventional logging analyses, the layers of the earth are considered to be non-magnetic, which results in $\mu = \mu_0$. With the magnetic permeability being held constant, $\bar{B}$ and $\bar{H}$ are simply proportional to each other and have no significant difference.

In induction logging, as mentioned earlier, two types of current are present. The first is the transmitted current that is generated within the loop source. The second is the induced eddy currents that circulate within the geologic formation. The distinction between the two types of currents is described by the following:

$$\nabla \times \bar{H} = \bar{J} + \bar{J}_s, \tag{2.8}$$

where $\bar{J}_s$ is the current density flowing within the loop source. Since $\bar{J} = \sigma \bar{E}$, Equation (2.8) can be rearranged as shown here:

$$\nabla \times \bar{H} - \sigma \bar{E} = \bar{J}_s. \tag{2.9}$$

Since the current energizing the coil of the transmitter is presumed to be sinusoidal, the equations involving the various field quantities are time dependent. This time dependence can be described by a factor $e^{(-i\omega t)}$. To incorporate this factor into the Maxwell equations, Equation (2.6) is first substituted into Equation (2.2):

$$\nabla \times \bar{E} + \frac{\partial \mu \bar{H}}{\partial t} = 0. \tag{2.10}$$

The next step is to add the time dependence factor and take the partial derivative. The resulting equation is:

$$\nabla \times \bar{E} - i\omega\mu \bar{H} = 0. \tag{2.11}$$

With the time dependence now accounted for, the governing Maxwell equations as applied to induction logging, now formulated in the frequency domain, are as follows (Moran and Kunz, 1962):

$$\nabla \times \bar{E} - i\omega\mu \bar{H} = 0.$$

$$\nabla \cdot \bar{E} = 0,$$

$$\nabla \times \bar{H} - \sigma \bar{E} = \bar{J}_s.$$

$$\nabla \cdot \bar{H} = 0.$$

It is important to note the $\nabla \cdot \bar{E} = 0$ because the layers in the Earth model are horizontal while the Tx loop axis is vertical. Due to this orientation, the eddy

currents flow in horizontal loops and do not cross layer boundaries, hence no charges are deposited on the layer boundaries. If this were not the case, then it would be required that $\nabla \cdot \bar{E} = \frac{\rho}{\varepsilon}$, where ρ is the volume charge density in units of $\mathrm{C/m^3}$ and ε is a scalar parameter without physical significance, but having the same units and numerical value as the dielectric constant or permittivity of free space.

The induction response of a logging tool is conveniently transformed into an apparent conductivity. The latter is the conductivity that would be recorded by an induction tool if the surrounding geologic formation was homogeneous. To determine the apparent conductivity of a heterogenous formation, the induced voltage in the receiver coil must first be found. Induced voltage is calculated by Moran and Kunz (1962) for a receiver coil of R turns wrapped around a mandrel of radius a by the following:

$$V = Real\{2\pi a R E_\phi\}, \tag{2.12}$$

where V is the voltage induced in the receiver coil and E_ϕ is the azimuthally-directed electric field. Once this voltage has been measured by the receiver, apparent conductivity, σ_a can be found using the following equation:

$$\sigma_a = \frac{V}{K}, \tag{2.13}$$

where K is a sensitivity factor specific to the particular logging tool under consideration. This sensitivity factor is derived from the geometry and other parameters of the logging tool as follows:

$$K = \frac{\omega^2 \mu^2 \pi a^4}{4L} I, \tag{2.14}$$

where L is the transmitter-receiver spacing, ω is the operating frequency, and I is the current in the transmitter coil (Moran and Kunz, 1962).

It is computationally more convenient to use the vertical magnetic field B_z instead of the azimuthal electric field E_ϕ in Equation (2.12) for the calculation of apparent conductivity. Therefore, E_ϕ should be cast in terms of the magnetic field. Faraday's integral law relates the magnetic field to the electric field by the following equation:

$$\oint_L \bar{E} \cdot d\bar{l} = -\int_S \frac{\partial \bar{B}}{\partial t} \cdot dA, \tag{2.15}$$

which states that the integral of the electric field around a closed circuit L is equal to the time rate of change of the flux of the magnetic field through the surface S bounding the area, A of the circuit (Hill, 2010). Assuming the Rx loop is small enough that the magnetic field is uniform over the area, A and given the parameters of a simple induction tool, Equation (2.15) can be written as:

$$\bar{E} = \frac{-i\omega A}{2\pi a} B_z. \tag{2.16}$$

Equation (2.16) can now be substituted into Equation (2.12) to obtain the voltage induced in the receiver coil in terms of B_z. This substitution yields the following equation:

$$V_R = \omega A \, Imag\{B_z\}, \tag{2.17}$$

where $Imag(B_z)$ is the imaginary or out-of-phase component of the magnetic field. Equation (2.17) is used in Equation (2.13) for finding the apparent conductivity of the formation.

2.2 Skin Depth

One of the governing physical attributes that Moran and Kunz (1962) take into quantitative account is the skin effect. The skin depth determines how deeply the induced currents penetrate into the geologic formation. The skin depth is influenced by frequency and the formation conductivity. The skin depth can be found using the following equation:

$$\delta = \sqrt{\frac{2}{\omega\mu\sigma}}. \tag{2.18}$$

In the equation above, δ is the skin depth measured in meters (Moran and Kunz, 1962). The physical meaning of the skin depth is that it describes the characteristic length scale of attenuation as an electromagnetic field diffuses into a conductive medium.

2.3 Geologic Roughness Parameter

By convention, in forward modeling a piecewise smooth spatial distribution of electrical conductivity is used to characterize the geologic subsurface. This is problematic given that geologic formations generally contain some measure of

roughness spanning a huge range of length scales (Everett, 2009). The pattern of spatial heterogeneity normally differs from length scale to length scale. In order to account for this hierarchical spatial variation in electrical conductivity throughout a geologic formation, a spatially uniform roughness parameter, β is introduced. The motivation for the roughness parameter is based on the statistical behavior of a random walk through a disordered medium, as originally described by Scher and Montroll (1975).

The geologic roughness factor is used herein to symbolize fractures in the subsurface (Ge et al., 2012). This factor is introduced as a slight modification to the equation for a loop response at harmonic transmitter frequency ω, current I, and loop radius a, given below:

$$E_s(\rho,\omega) = -i\omega\mu_0 Ia\int_0^\infty \frac{e^{-\gamma_0 z}}{\gamma_0}\frac{Z^1}{Z_0+Z^1}J_1(\lambda a)*J_1(\lambda\rho)*\lambda d\lambda. \tag{2.19}$$

In the above equation, $E_s(\rho,\omega)$ is the secondary electric field at some source-receiver separation distance ρ, and J_1 is a first order Bessel function (Decker et al., 2009). The focus of this equation, in relation to the β parameter, is on the propagation constant γ. Classically, this value is defined by:

$$\gamma = \sqrt{\lambda^2 + i\omega\mu_0\sigma_i}. \tag{2.20}$$

However, to describe the roughness of the layer, the equation is modified in the following way:

$$\gamma = \sqrt{\lambda^2 + (i\omega)^{1-\beta}\mu_0\sigma_i}. \tag{2.21}$$

It is easily seen that if the β parameter is set to 0, the equation reduces to the original solution for a non-fractured layer (Decker et al., 2009). For further details on the physical motivation for the roughness factor β as it applies to CSEM data interpretation, see Weiss and Everett (2007).

2.4 Original SEATEM Program

The computer program used in this study to generate synthetic induction logs was written by the thesis advisor in the Fortran programming language. The program is a modification of a 3-D marine controlled-source electromagnetic induction code, called Seatem, based on the finite element method. In turn, Seatem is based on the $(\bar{A},\psi)$ numerical modeling algorithm described by Badea et al. (2001) in which $\bar{A}$ is the magnetic vector and ψ is the electrical scalar potential. The original coding, prescribed a horizontal electric dipole located on the seafloor transmitting at a single frequency. The response of a conducting wholespace as the background provides the driving term for the computed secondary Coulomb-gauged electromagnetic potentials. In the original model a non-magnetic, isotropic seafloor is considered, but it can contain 3-D conductive structures with irregular bathymetry.

For ease of use, the Seatem code is broken up into modules that are run sequentially. The first module is a mesh generator. This subprogram reads in a certain model geometry and provides an output in the form of a tetrahedral

mesh file. The geometries that are currently available in this module include a homogenous earth with a buried target, and a layered earth.

The second module of the Seatem code contains two main components. The first is a routine that assembles the finite element matrix and the right-side vector. This matrix is populated using the resistivity of each tetrahedron and the geometry of each vertex in the mesh file. The right-side vector contains information about the driving primary potentials. The second component of this module is a quasi-minimal residual solver that is used to evaluate the matrix equations. This solver outputs the vector and scalar secondary potential values at each vertex of the 3-D mesh. This procedure is repeated for each of the specified transmitter operating frequencies.

The third module of Seatem involves post-processing of the finite element solution. This module differentiates the potentials that were computed in the second module, thereby deriving the electric or magnetic fields along a specified measurement profile. In this step, any component of the electric and magnetic fields can be derived on any set of arbitrary nodes.

The final module in the Seatem code takes the frequency-domain electric field, found in the third module, as input and computes a step-off or transient response in the time domain. This step is performed using a cosine transform.

3. METHOD

3.1 Layered Earth Model

The environment used for the induction log simulations is a layered Earth model. The model consists of six layers that are assigned different thicknesses and conductivities based on the desired induction log to be produced. A simple diagram of the layered Earth model can be seen in Figure 3.1.

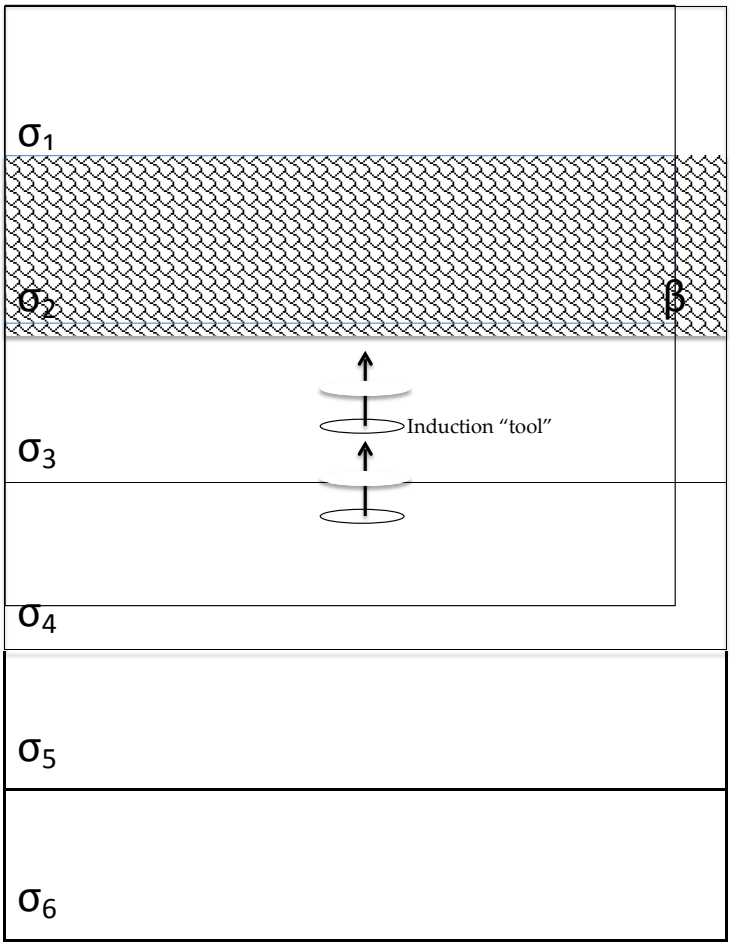

Figure 3.1. Layered Earth model used to produce synthetic induction logs.

The downhole tool, used to generate the synthetic log, is a two-coil vertically oriented Tx-Rx pair with a fixed separation. The computer program allows the Tx to operate at various frequencies. The tool is moved vertically through the Earth model and apparent conductivity readings are computed at specific logging points to generate complete synthetic logs of the layered Earth model. After a synthetic log is generated for a specified geologic formation, the geologic roughness parameter β is applied to one of the layers and a new synthetic log is calculated to show its effects.

3.2 Modified SEATEM Program

To accommodate induction log simulation, multiple changes to the original Seatem code are necessary. The first major change is to the source of the electromagnetic induction. In the original Seatem program, the source is a horizontal electric dipole. This source must be converted to a vertical loop source that is paired with a receiver loop in the same orientation. An additional change is also necessary when discussing the source. In the original code the source is a Tx on the seafloor at a fixed location operating at a single fixed frequency, paired with seafloor Rx electric dipoles located at variable offsets. In the altered Seatem code the single Tx-Rx pair has a fixed separation and is moved along a vertical profile through the subsurface taking measurements at predetermined logging points.

The second change to the original Seatem code involves the surrounding environment. The code is transformed from a seafloor environment, with its overlying water column and isotropic seafloor, to a layered Earth environment with geologic formations of varying conductivities situated both above and below the transmitter.

The final change to the Seatem code after it has been converted to a logging code is the implementation of the geologic roughness factor. Once the code modification is in place, a β roughness value from 0.0 to 1.0 can be assigned to any of the layers in the model space before initiating a synthetic logging calculation.

3.3 Program Specifications

The mesh that is generated by the modified Seatem program, applicable to the logging environment, is cylindrical and spans a vertical distance of 240 meters. The mesh consists of 80 layers that are separated by 3 meter spacing. The total number of tetrahedra that make up the synthetic geologic environment is 61,440. The logging tool has fixed Tx-Rx separation of 4 meters. The skin depth at each logging point is usually between 25-75 meters, corresponding to layer conductivities between 0.1-0.5 S/m and operating frequencies of 200 Hz to 1 kHz. The computational cost of running the program is quite low for finite element modeling since the Tx and Rx loops are located in the center of the mesh, far from its outer boundary, and the Tx-Rx separation is much less than

one skin-depth. The QMR solver typically converges in about 150 iterations. When implementing a single operating frequency, a synthetic logging response at any given point can be computed in 30-45 CPU-seconds. With user input playing a significant role in the logging program, complete synthetic logs can be produced in 2-3 hours of wall-clock time.

4. DATA ANALYSIS

The first synthetic log generated by the modified Seatem program is shown in Figure 4.1. This log was created to validate the changes made to the original Seatem program. The Earth model consists of six layers that vary in conductivity from 0.1 S/m to 0.5 S/m. The downhole tool has a Tx-Rx separation of 4 meters and operates at three different frequencies: 200 Hz, 500 Hz, and 1 kHz. A logging response was calculated every 2-3 meters for each operating frequency to generate this synthetic induction log. The logging point is defined as the midpoint between the Tx and Rx loops, i.e. the center of the logging tool. The resulting log is encouraging and demonstrates the reliability of the modified Seatem program. The synthetic logs for the three operating frequencies are similar and provide a good, albeit smooth, estimate of the actual conductivity, which is denoted as the black piecewise-constant curve in Figure 4.1. There is slight variation between the logs for different operating frequencies especially within the most conductive layer at 0.5 S/m, but in general the logs appear to accurately represent the layer conductivities of the Earth model. The synthetic log also exhibits some of the expected characteristics that are seen in actual induction logs. For example, the traces peak in the center of the layers and show smooth variations across the boundaries between layers. This is common in induction logging applications and supports the supposition that the modified Seatem program can generate accurate synthetic logs.

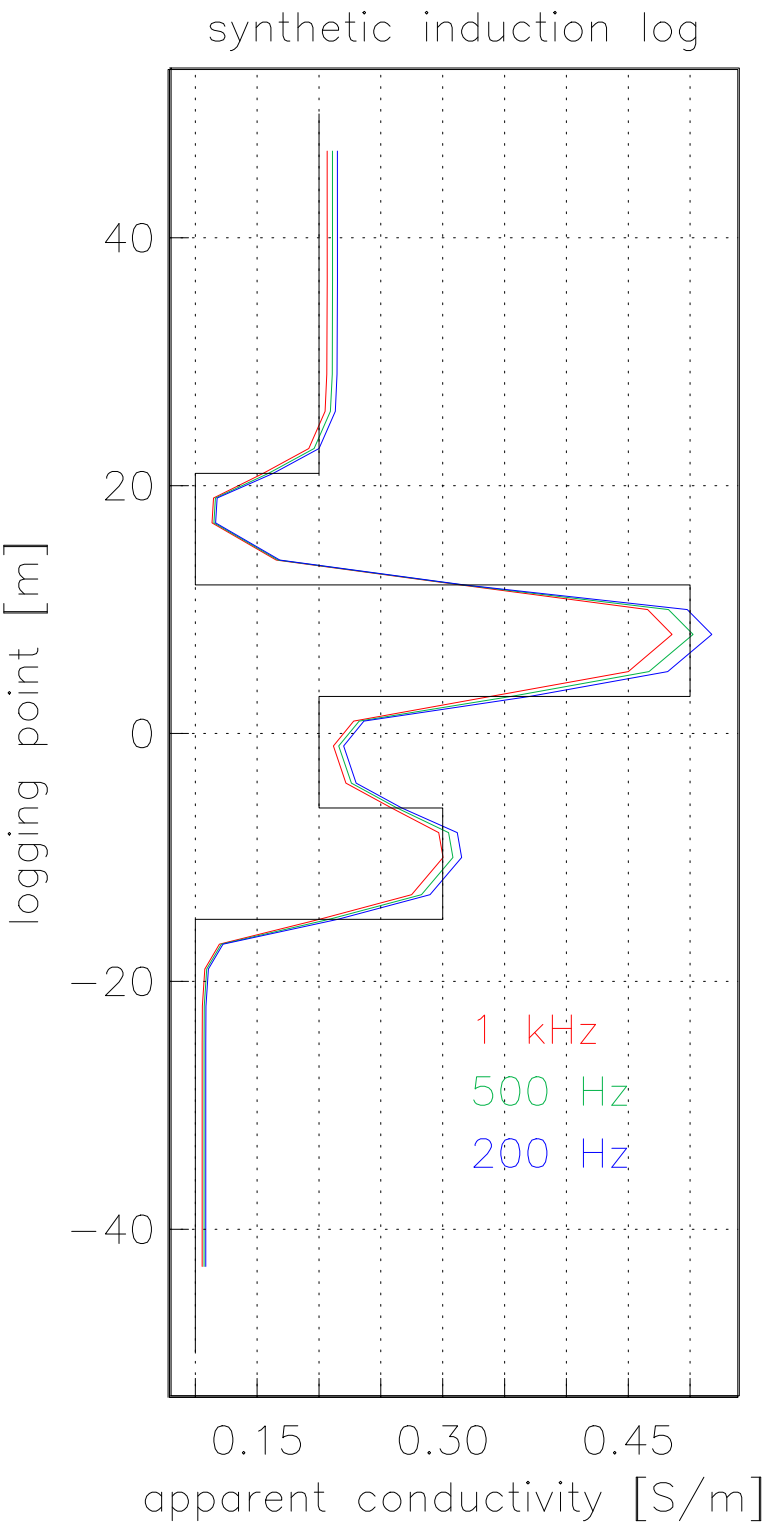

Figure 4.1. Synthetic induction log with three operating frequencies created to validate the modified Seatem program.

4.1 Thinning Bed Analysis

The next set of synthetic logs to be calculated is based on a thinning conductive bed. The Earth model was specified with six layers and these were assigned conductivities ranging from 0.1 S/m to 0.4 S/m. In this analysis the thickness of the bed assigned to the highest conductivity was gradually stepped down in size to observe the effects of a thinning bed on an induction log. The thickness of the conductive layer in the initial run was set to 9 meters, then moved down to 6 meters, and a final log was generated for a 3-meter-thick conductive layer. The corresponding computed logs can be seen in Figure 4.2, Figure 4.3, and Figure 4.4. The logging points are 3 meters apart and the operating frequencies used are 200 Hz, 500 Hz, and 1 kHz.

In the initial log, seen in Figure 4.2, the three responses again trend closely together, as earlier seen in Figure 4.1. The measured responses closely track the actual conductivity. However, when the conductive layer is thinned to 6 meters, as shown in Figure 4.3, the three log responses smooth over the peak within the conductive layer and consequently underestimate its actual conductivity. A further change between this log and the previous one is seen in the surrounding layers. The traces in the surrounding layers show increased rounding at the edges and begin to more accurately track the layer boundaries. When the bed is thinned to its final value of 3 meters in thickness, as shown in the log in Figure 4.4, the differences seen in the first two logs are amplified. The apparent conductivity in the layer becomes further underestimated and the log signature

spikes. The rounding of the edges in the surrounding layers is also increased in this log which shows that the computer program more accurately characterizes these layers. It is important to note that the Tx-Rx spacing of the induction tool is 4 meters, making it impossible for the transmitter and receiver to both be in the thin layer of interest at any single logging point. This could be the reason behind the spiky appearance of the log within the thin conductive layer. Despite the changes in the three logs, the operating frequency does not appear to be a factor in understanding these thinning bed phenomena. The logs associated with the three frequencies used in this analysis track closely to one another.

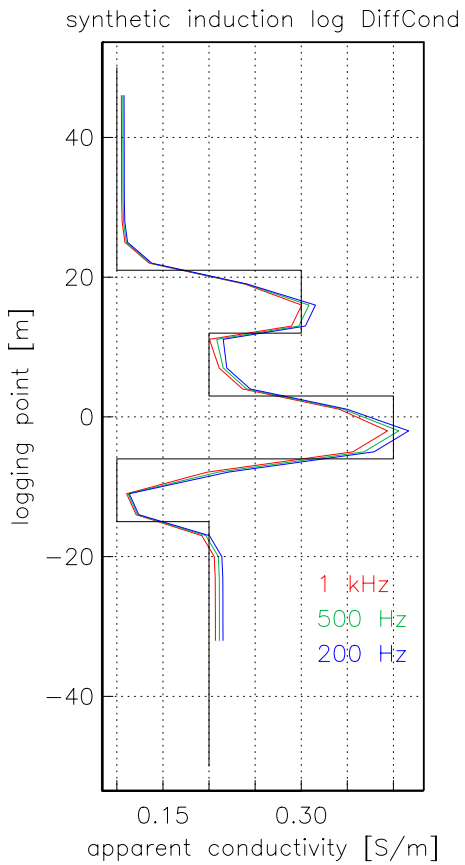

Figure 4.2. Synthetic induction log for thinning bed analysis. Conductive layer in this first simulation is 9 meters thick.

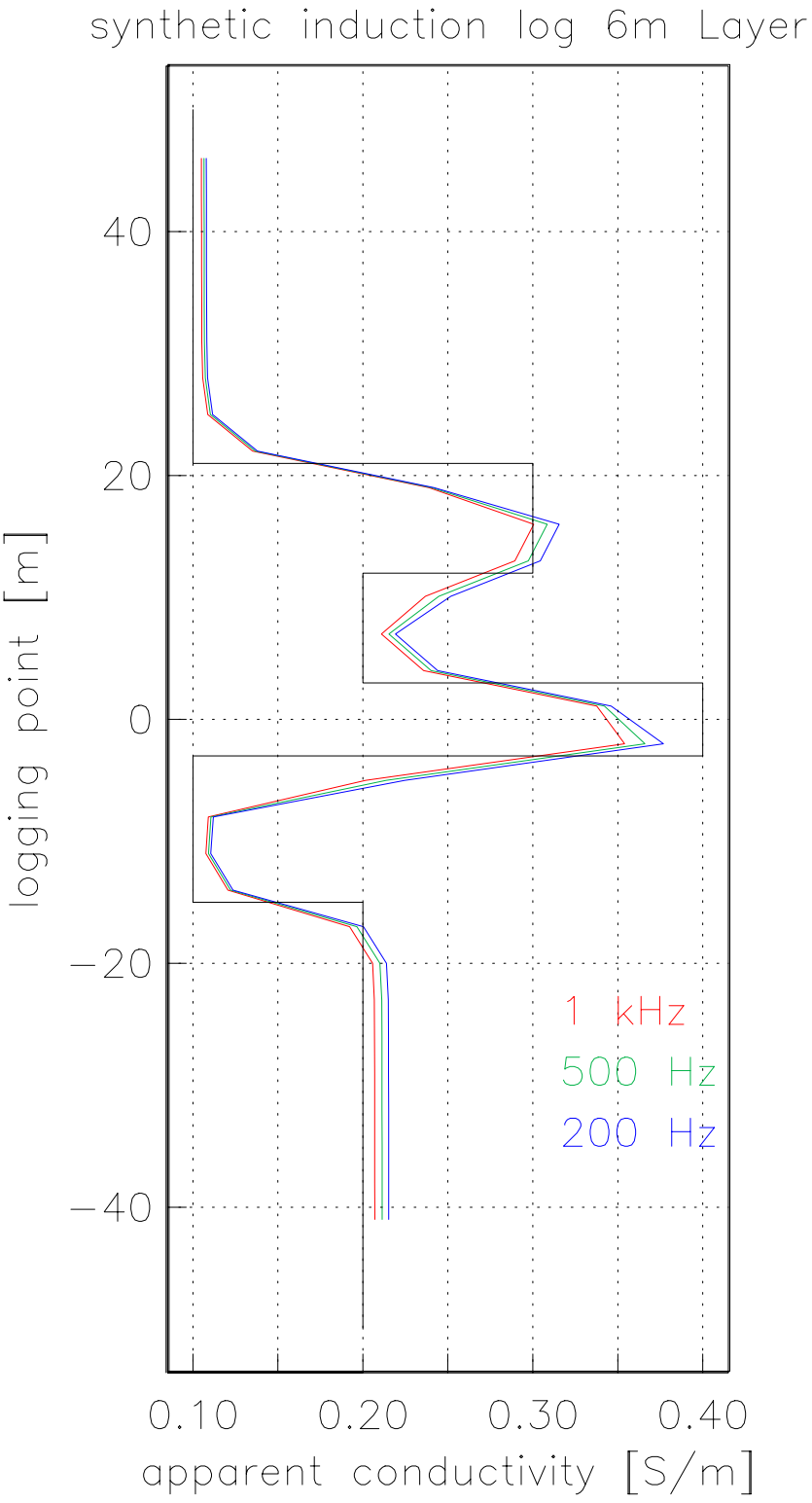

Figure 4.3. Synthetic induction log for thinning bed analysis. Conductive layer in this second simulation is 6 meters thick.

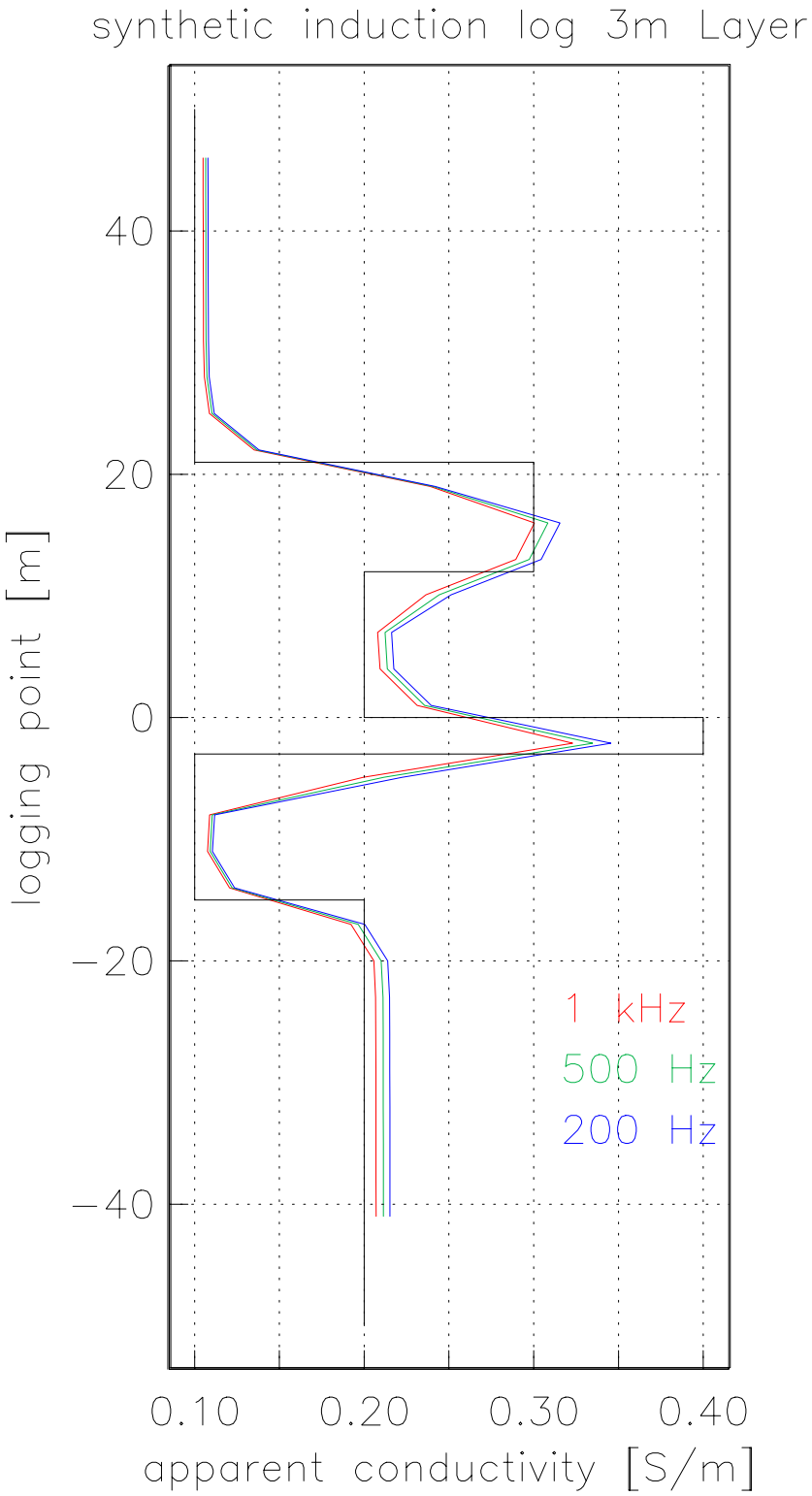

Figure 4.4. Synthetic induction log for thinning bed analysis. Conductive layer in this final simulation is 3 meters thick.

4.2 Geologic Roughness Analysis

After checking the program and observing the effect of thinning beds on synthetic induction logs, a non-zero roughness parameter β was applied to one of the geologic strata within the layered Earth model. Given the relative insensitivity of the operating frequency discovered in the previous log simulations, a single operating frequency of 1 kHz was selected for the analysis of the effect of the roughness parameter.

4.2.1 Fractured Resistive Layer

The first evaluation of the effect of the roughness parameter on a synthetic induction log was made by applying different values of β to a resistive layer. The same layered Earth model was specified as the one earlier used to generate the log shown in Figure 4.1. The model contains six layers that are each 9 meters thick and have conductivities ranging from 0.1 S/m to 0.5 S/m. As previously stated, the operating frequency for this log was set to 1 kHz, because in the previous logs the operating frequencies was not a sensitive factor and the 1 kHz reading provided accurate results. The resulting induction log for the model containing the rough resistive layer can be seen in Figure 4.5. Three different β values were assigned to the 0.1 S/m resistive layer and a log was generated for each value. The β values used were 0.0, 0.2, and 0.4. The log shows interesting results and shares some attributes with the previously described thinning-layer

logs. First, the log shows that as the β value is increased in the resistive layer, the logging response increasingly underestimates the actual conductivity. Another characteristic of the observed synthetic log signal is that the response close to the rough-layer boundaries changes slightly as β is increased. The edges of the curve just above and below the boundary grow more distinct as the roughness parameter increases. This suggests that the presence of a rough geologic formation makes the log measurements close to the formation's boundary more accurate.

Since the log shown in Figure 4.5 shares many attributes with the thinning bed logs, the next step in the investigation of the geologic roughness parameter is to thin the layer of interest. Figure 4.6 is the result of the same model used to generate Figure 4.5 with the only difference being that the resistive layer is only 6 meters thick. The model of the thin, resistive layer, containing fractures, produces fairly predictable results. The log responses in the thin resistive layer begin to spike, similar to the responses seen in Figure 4.3. The underestimation seen in the thick layer for this model is not as severe in the thin, fractured layer. This result is expected as a similar observation was made during the thinning bed analysis. This observation is that the thinning of the bed will smooth out the induction log response and, if the bed is thin enough, the downhole tool could miss it altogether.

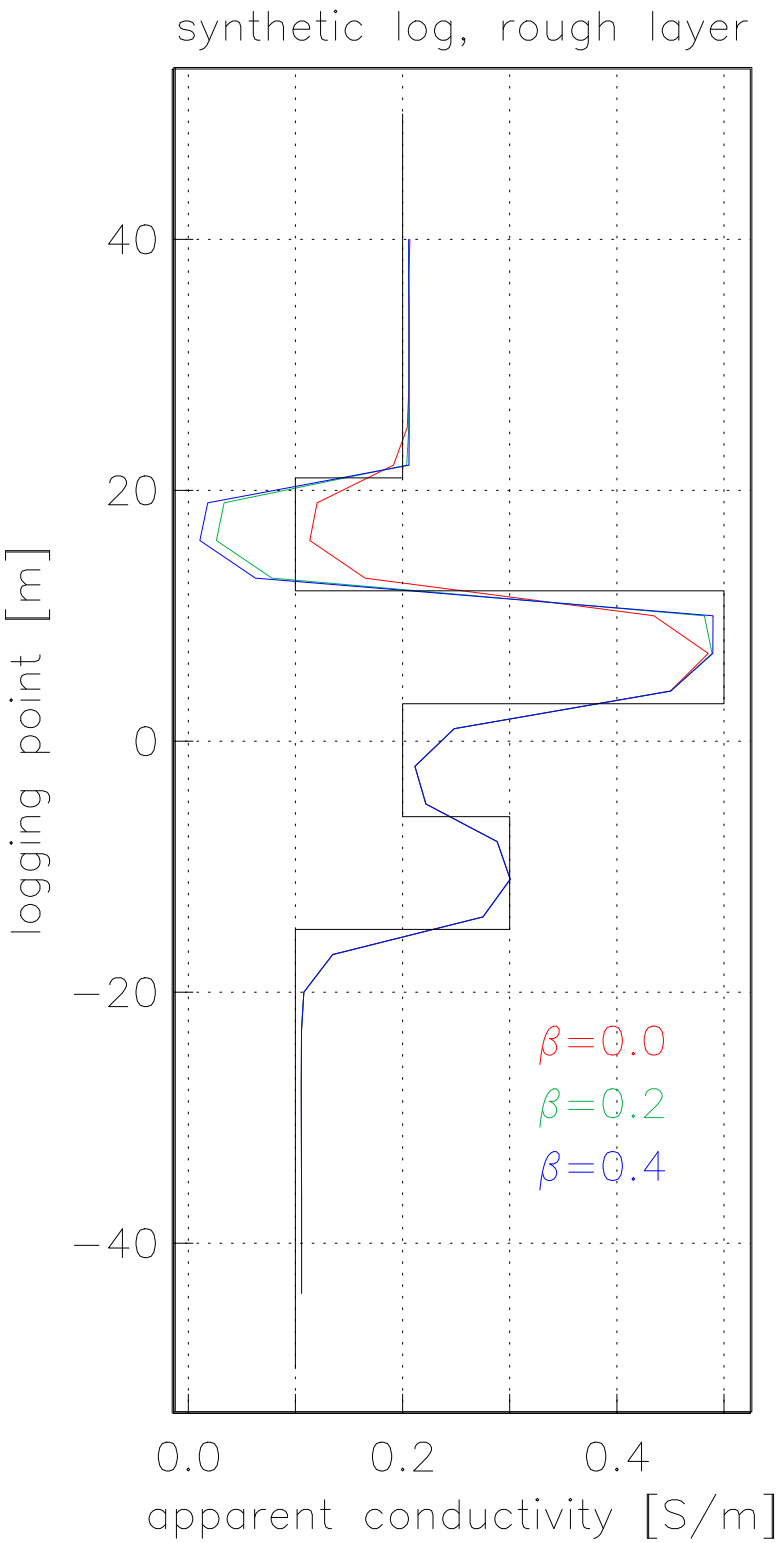

Figure 4.5. Synthetic induction log of a resistive layer with different values of geologic roughness.

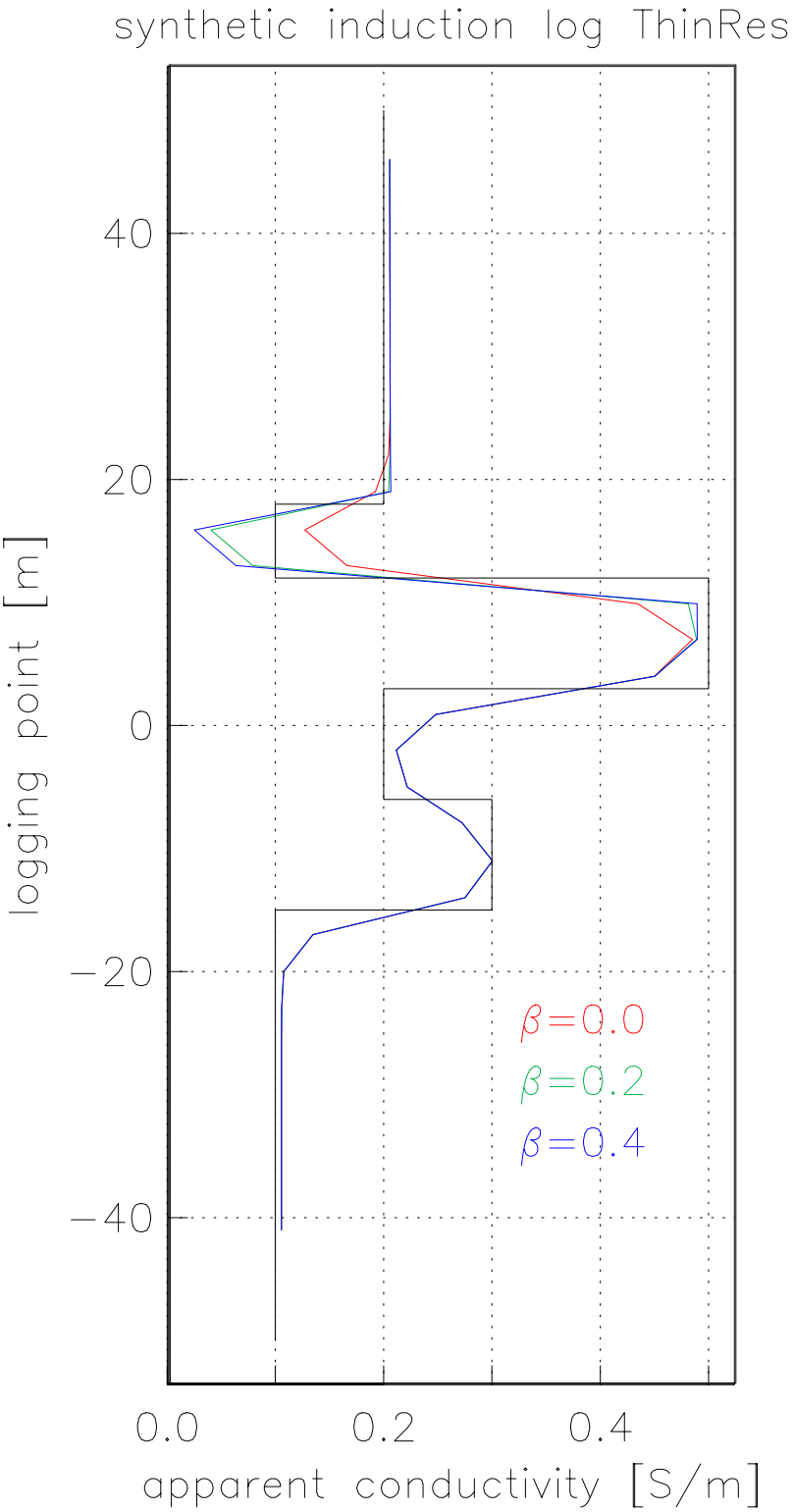

Figure 4.6. Synthetic induction log of a thin resistive layer with different values of geologic roughness.

4.2.2 Fractured Conductive Layer

With the logging response of a fractured resistive layer observed, the next step in the research project was to generate logs with a focus on a fractured conductive layer. The same model parameters used to generate the layered Earth model in the analysis of the fractured resistive layer were used in the analysis of the fractured conductive layer. The formation of interest in this analysis is the 9 meter thick, 0.5 S/m conductive layer. Three logs were run for the different β values of 0.0, 0.05, and 0.075. The logs for this model can be seen in Figure 4.7 and drastically different results are evident compared to earlier results on the resistive counterpart. One major difference is that the apparent conductivity measurement is much more sensitive to the β parameter. As the β value is increased, the measured apparent conductivity is increasingly underestimated, as in the previous models. The most significant difference here, however, is that the amount at which the measured response drops in relation to a small increase in β is much larger than in the previous examples. When the log was calculated for $\beta = 0.075$, the underestimation for conductivity was so extreme, that the conductive layer was almost undetected by the logging tool. One characteristic this log does share with the resistive case is that the layer boundaries around the conductive layer produce a log signature that attempts to better image the boundary interface.

As in the case with the resistive layer analysis, the next step was to shrink the conductive layer for further analysis. The layer thickness was changed from 9

meters to 6 meters. The synthetic log of the thin conductive, fractured layer is shown in Figure 4.8. The effects caused by the thinning of the conductive bed are comparable to the case of the thinning of the resistive bed. The log responses in Figure 4.8 show the same underestimated conductivity values as seen in Figure 4.7, but to a greater extent. The curves begin to smooth out as the layer gets thinner. In the β=0.075 log, the thin conductive layer almost appears as noise in the data set. The strong reading that should be present in such a highly conductive layer is absent in this case.

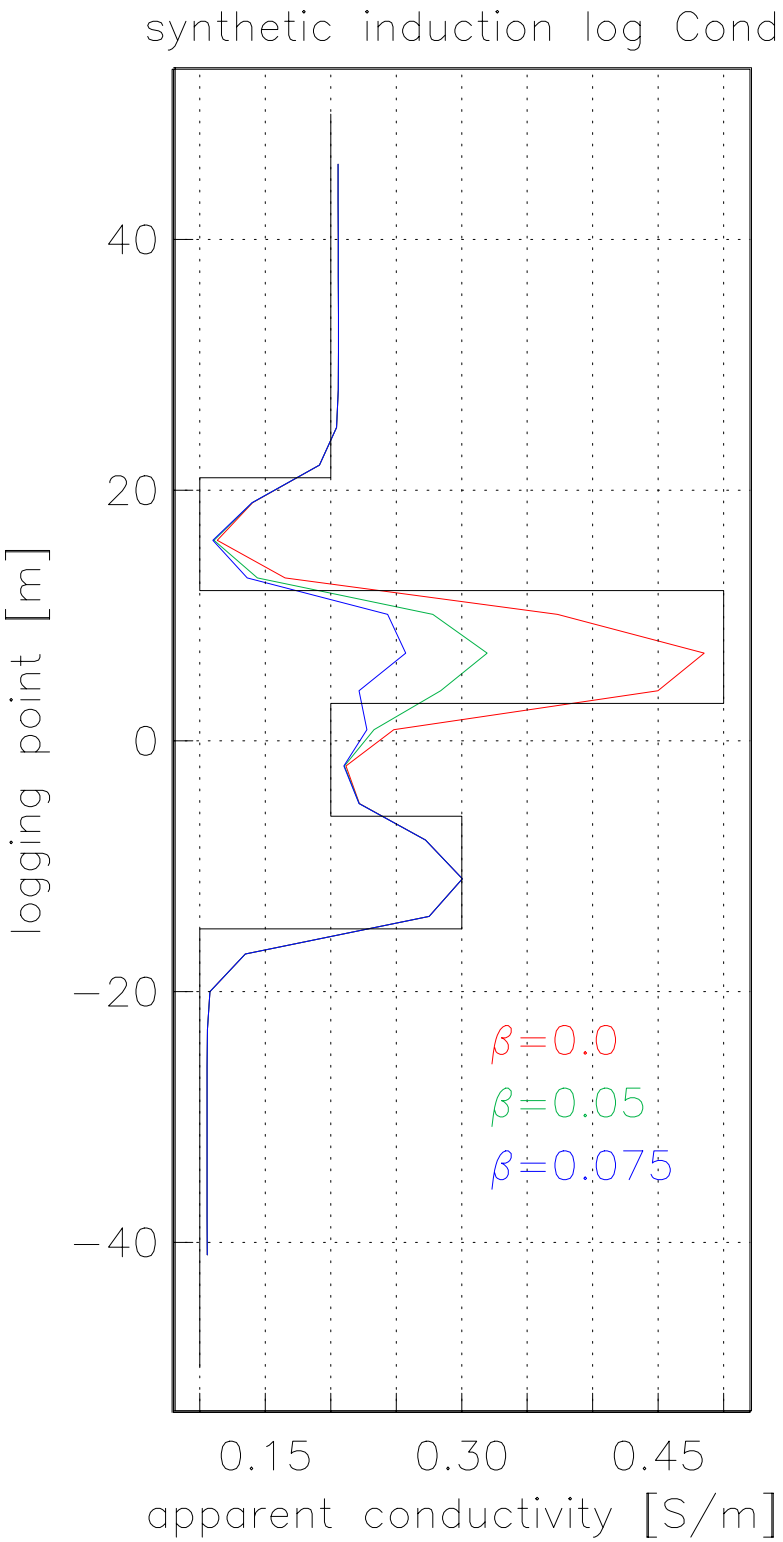

Figure 4.7. Synthetic induction log of a conductive layer with different values of geologic roughness.

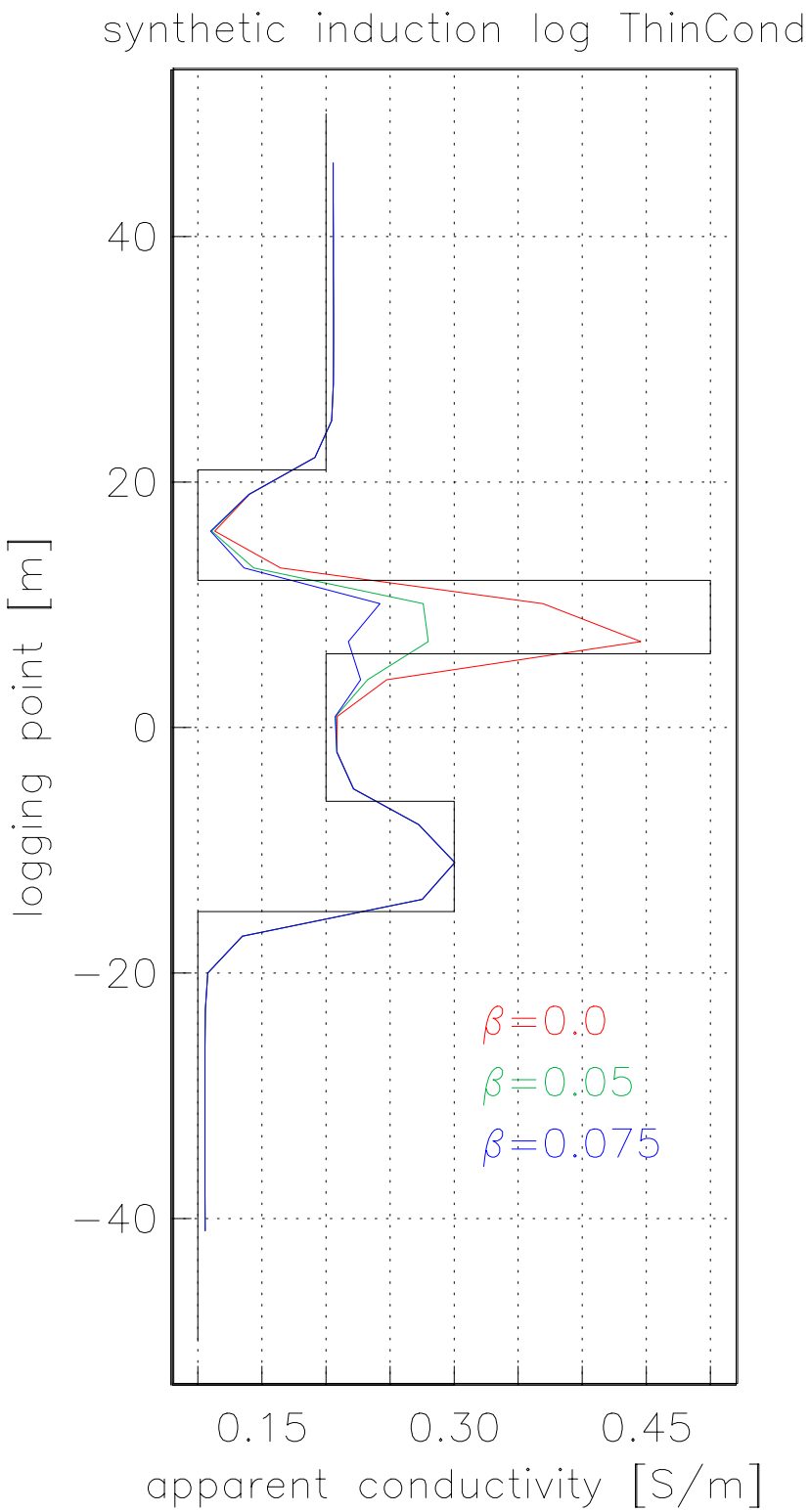

Figure 4.8. Synthetic induction log of a thin conductive layer with different values of geologic roughness.

5. CONCLUSION

The geologic roughness parameter β is shown in this research project to have a significant effect on synthetic induction logs. The fractures in the geologic formations interact with the electromagnetic fields in such a way that reduces their apparent conductivity. In a fractured resistive layer, the calculated logs from the Seatem program underestimate the actual conductivity of the layer. As the unit became more fractured, the logging measurements further underestimated the conductivity. The same result occurred in the conductive layer analysis, but to a much greater extent. Even a small increase in the value of roughness leads to severe underestimation in the apparent conductivity of a synthetic log. The layer is almost unrecognized in the log as the roughness reaches β=0.1, in the conductive case.

Another important impact of the geologic roughness on synthetic induction logs is shown when characterizing the layer boundaries of the fractured strata. It is shown in the logs that, while underestimation of apparent conductivity is evident in the fractured layer, the log signature in the surrounding layers appears to become more accurate. The log responses close to the boundary layers show less smooth variation in the transition zones and become more angular within the transition zone. The better reproduction of the true conductivity at the layer boundaries suggests that the strong change in the electromagnetic field that is occurring within the fractured unit has an effect on the log signature in its surrounding layers.

5.1 Importance

The research project is a step in the right direction for better understanding the geophysical signature of fractures in the subsurface. Induction logging is a very powerful tool that provides valuable information to industry and researchers. Any way to further develop this proven method is beneficial. Whether it is characterizing hydro-fracking jobs or evaluating formations in exploration, the acquisition and interpretation of induction logging is very important. The technology is relatively inexpensive and if the applications for this tool are broadened there is no limit on how helpful it could be in solving our energy demands and enabling environmental impact studies.

5.2 Future Research

Given the encouraging results of this research project, there is a wide array of areas where future research could develop better induction logging techniques. The main focus for future research should be on the further development of the Seatem logging program. Many different aspects of induction logging can be added to the code to better reflect real world practices in induction logging. For example, the addition of a borehole to the model, along with a fluid invasion zone, should be considered in the future. Also, tool corrections like eccentricity and accounting for the composition of the mandrel can fairly simply be implemented into the Seatem code. To reflect the present day practice of

horizontal drilling, many of the same models in this research project can be run to accommodate deviation of the borehole. The current coding can support deviation up to about 85 degrees. Another section of the Seatem program that can be altered is the Tx-Rx orientations. This addition is more computationally intensive than the other changes suggested in this section. All of the previously mentioned improvements to the Seatem code will created a more sophisticated logging program that can handle more complex models. Once the program is so modified, it would become beneficial to compare synthetic logs from the program to actual logs from field data that share similar physical characteristics.

REFERENCES

Badea, E., M. E. Everett, G. A. Newman and O. Biro. (2001). Finite element analysis of controlled-source electromagnetic induction using gauged electromagnetic potentials, *Geophysics* **66**, 786—799.

Decker, K. T., M. E. Everett. (2009). Roughness of a layered geologic medium and implications for interpretation of the transient electromagnetic response of a loop source. *SAGEEP* **22**, 188.

Doll, H. G. (1949). Introduction to induction logging and application to logging of wells drilled with oil base mud. *Petroleum Development Technology*: *Transactions of the American Institute of Mining and Metallurgical Engineers*, **186,** 148-162.

Everett, M. E. (2013). *Near-surface applied geophysics*, Cambridge University Press, New York, NY.

Everett, M. E. (2009). Transient electromagnetic response of a loop source over a rough geological medium, *Geophysics* **177**, 421-429.

Ge, J., M. E. Everett, and C. J. Weiss. (2012). Fractional diffusion analysis of the electromagnetic field in fractured media Part I: 2D approach. *Geophysics*, **77.4,** WB213-WB218.

Grant, F. S., G. F. West. (1965). *Interpretation Theory in Applied Geophysics*, McGraw-Hill Book Co., New York, NY.

Hill, E. S. (2010). Rephrasing Faraday's Law, *The Physics Teacher* **48**, 410-412.

Moran, J. H., K. S. Kunz. (1962). Basic theory of induction logging and application to study of two-coil sondes. *Geophysics*, **27.6** 829-858.

Scher, H., E. W. Montroll. (1975). Anomalous transit-time dispersion in amorphous solids, *Phys. Rev. B* **12**, 2455-2477.

Schlumberger. (1969). *Log interpretation principles*, Schlumberger Limited, New York, NY.

Wang, T., X. Tang, L. Yu, B. Kriegshauser, O. Fanini, and G. Ugeto. (2005). Characterizing fractures with multicomponent induction measurements, *Petrophysics* **46**, 42-51.

Weiss, C. J., M. E. Everett. (2007). Anomalous diffusion of electromagnetic eddy currents in geological formations, *Journal of Geophysical Research* **112**, B08102.